Congresso de Métodos Numéricos em Engenharia 2015
Lisboa, 29 de Junho a 2 de Julho, 2015

A QUALITATIVE ANALYSIS OF FLUID SIMULATION USING A SPH VARIATION

André L. Vieira e Silva[1]*, Mozart W. Almeida[1], Caio J. Brito[1], Veronica Teichrieb[1], José M. Barbosa[2] and Cesar Salhua[2]

1: Centro de Informática
Universidade Federal de Pernambuco
Av. Jornalista Anibal Fernandes, s/n, Cidade Universitária (Campus Recife), 50740-560, Recife, Pernambuco, Brazil
e-mail: {albvs, mwsa, cjsb, vt}@cin.ufpe.br web: http://www.cin.ufpe.br/voxarlabs

2: Departamento de Engenharia Mecânica
Universidade Federal de Pernambuco
Av. Prof. Moraes Rego, 1235, 50670-901, Recife, Pernambuco, Brazil
e-mail: jmab13@gmail.com, csalhua@hotmail.com

Keywords: XSPH, Analytical Method, Weakly Compressible, Fluid Simulation

Abstract *Fluid simulation using meshless methods has increasingly become a robust way to solve mechanics problems that require dealing with large deformations, in that way, it is briefly shown what the main challenges and advances in the area are. The smoothed particle hydrodynamics (SPH) is then introduced. One of its variations is the Weakly Compressible SPH (WCSPH), which was used as a baseline to implement the method used in this work, called XSPH. Finally, four usual test cases of fluid simulation are analyzed: the lid-driven cavity flow, the dam break, the Poiseuille flow and the elliptic drop. The analysis concluded that the method used in this work performs at least as well as the most reliable and accurate models, and in some aspects performs better.*

1. INTRODUCTION

Some computational mechanics problems require dealing with large deformations, including those related to solid molding, casting and for the simulation of manufacturing processes [1]. Furthermore, for simulating fluids – the main focus of this work – there are also requirements for even larger deformations.

Although more accurate and well consolidated, the conventional methods (finite element, finite differences etc.) have some problems when dealing with such required deformations, as those methods rely on meshes, which cannot handle the moving discontinuities efficiently. According to [2], the best approach for mesh-based methods dealing with this kind of problem is remeshing every iteration step of the simulation in order to keep the mesh discontinuities

coincident through the entire simulation. Evidently, all this effort may generate difficulties such as accuracy degradation and computational overload.
Justified by those problems, the meshfree methods have been very useful as an alternative approach of dealing with such large discontinuities, as there is no explicit connection between the elements of the system, the particles. Besides that, others advantages are easily recognizable in comparison to those conventional methods, such as discretization of complex geometry or the refinement of particles that is done easier than mesh refinement.
Meshless methods use discrete elements, called particles, characterizing the system state and its evolution through time. Each particle carries a set of physics quantities, such as mass, velocity, position and any other related to the problem being simulated. This Lagrangian characteristic is important as every particle quantity can be easily tracked along the simulation, making it advantageous over Eulerian mesh-based methods.
One of the most known meshless methods nowadays is the Smoothed Particle Hydrodynamics (SPH), which was designed over three decades ago by Lucy [3] and Gingold and Monaghan [4] and intended to astrophysics applications. Since then, there has been continuous improvements and adaptations of this original method in order to adequate it to the simulation of various kinds of physical phenomena.
As the particles are not connected explicitly by any edge, it is also possible to optimize some computational aspects of the simulation, such as by parallelization, using cluster technology or general purpose programming for graphics processor (GPGPU) techniques.
A good practice in Computational Fluid Dynamics (CFD) is the utilization of analytic solutions or experimental results of some simple known problems, in order to evaluate the correctness of the method developed.
Hence, in this work we used some of these solutions and experimental results found in the literature, presenting these evaluations and results obtained, in order to be able to tell if the chosen SPH methods are suitable for our purposes, which initially are related to accuracy and robustness of the simulation.
The next section presents major state-of-the-art works using the meshless approach focusing on the chosen method for this work. The section 3 introduces the mesh-free method used in this work, the SPH, showing its specific details. After that, the section 4 details the results obtained, making a numerical comparison through the use of each respective analytic solution. The section 5 discusses the next steps needed to improve the algorithm implemented and evolve robustness of the simulation, and concludes the work by stating the lessons learned by working with this technique.

2. RELATED WORK

In recent years, various authors [2][5][6] tried to present discussions and reviews always trying to classify the meshless methods by some inherent characteristics such as types of mathematical formulations or the various kinds of approximations.

Due to this somewhat lack of standardization in the area [7], and as it has been briefly mentioned in the previous section, in this one we will keep focus mostly on the development and recent advances of the SPH technique, more precisely on those applied to CFD problems, which by itself is already a vast area of study.

After being introduced to modeling astrophysical phenomena by [3] and [4], the SPH method has been vastly extended to model fluids and solids behavior, mainly under those aspects which could limit the applications simulated by mesh-based approaches.

The most straightforward adaptation to the original method is the application for weakly compressible fluids, in which for the calculation of pressure, an equation of state can be used as in the works of [8][9][10][11][12]. The main difference between the original method and the newer ones is the inclusion of boundary conditions [13][14][15].

The attempts to simulate incompressible fluids were achieved applying some techniques introduced by [16] and are extensively used in the works of [17][18][19][20]. These methods try to maintain the density of the system constant throughout the simulation by applying the projection method or modifying the equation of state, using a high value for the speed of the sound as mentioned by [21].

Some works on the literature propose explicit comparisons between weakly compressible and incompressible approaches [8][9][22].

Besides the compressibility factor present in the fluids, some other elements can be adapted to the kind of problem being studied, like the viscosity of the fluid, presence or absence of turbulence, type of smoothing function, among others.

Some works present results for adjustments in the viscosity according to the problem being focused [21][23][24][25][26]. For turbulent flows, some papers try to adapt known methods into the particles systems [27][28].

In order to explain the effects of the smoothing function on the simulations, some works compare and adapt some types of functions in order to evaluate accuracy and stability of the method [25][29][30][31][32].

Unfortunately, similarly to the other meshfree methods, the SPH suffers from two kinds of instability problems: the first one is related to instability at the boundaries, i.e., free surfaces, interaction with solids and so on [33][34][35][36][37][38]. The second problem is related to the interactions between the internal particles and is known as tensile instability.

Approaching the problem of boundaries, works like [39], [40] and [41] propose efficient ways of dealing with these problems. Another kind of boundaries that may suffer from instability problems is the interface between two different fluids in a multiphase scenario. The works from [42] and [43] illustrate how this must be approached. A vast number of papers focus on resolving the problem of tensile instability as well. The works of [26] and [44] exemplify some of these approaches.

3. SPH

The SPH method approach treats the continuum fluid as a finite number of particles. Each particle has properties as position, mass, density, velocity, pressure and a radius of action.

In the continuous form, a fluid flow can be defined using two equations describing the conservation of the mass (1) and of the momentum (2) [45].

$$\frac{d\rho}{dt} = -\rho\nabla \cdot v \tag{1}$$

$$\frac{d\vec{v}}{dt} = -\frac{1}{\rho}\nabla P + \frac{1}{\rho}\nabla \cdot \vec{\tau} + Fext \tag{2}$$

where ρ stands for density, t is the time, v is the velocity, P is the pressure, τ is the viscosity and $Fext$ represents the external forces in the system (e.g. gravity).
In the discrete form, any property A of a point with position x is formulated as a discrete convolution of a kernel function w as in (3) and the respective gradient (4).

$$A(x) = \sum_j A(x_j)\frac{m_j}{\rho_j} w(x - x_j, h) \tag{3}$$

$$\nabla A(x) = \sum_j A(x_j)\frac{m_j}{\rho_j} \nabla w(x - x_j, h) \tag{4}$$

where j is the particles index of each particle inside the kernel influence, x stands for the position of a particle, m is the mass of a particle.
A kernel function must be chosen taking some criteria in consideration:

1) The smoothing function is normalized
2) The kernel is symmetric
3) The function must have a compact support

This last property reduces the problem size to the radius of action of a particle, which is the smoothing length h multiplied by a scaling factor k:

4) W is non-negative throughout its domain
5) The smoothing value decreases with the distance to the particles in the center
6) The limit of the kernel function must approache the Dirac delta function

In this work, the cubic spline kernel (5) was chosen with a smoothing length of $2k$, where k is equal to the initial particle spacing [46].

$$w\left(\vec{r_i} - \vec{r_j}, h\right) = w(R, h) = \alpha_d \times \begin{cases} \frac{2}{3} - R^2 + \frac{1}{2}R^3 & 0 \le R < 1 \\ \frac{1}{6}(2 - R)^3 & 1 \le R < 2 \\ 0 & R \ge 2 \end{cases} \tag{5}$$

where $R = \left|\overrightarrow{r_i} - \overrightarrow{r_j}\right|/h$ and $\alpha_d = \frac{15}{7\pi h^2}$.
The density of a particle is usually calculated using the density summation equation (6) [47].

$$\rho_i = \sum_j m_j \, w_{ij} \tag{6}$$

This approach may not lead to an accurate result in case of a particle deficiency in the fluid free surface or near boundary, caused by the insufficient number of particles inside the truncated kernel. One way to improve the density calculation is to normalize the kernel in the density summation as in the formula (7) [32].

$$\rho_i = \frac{\sum_j m_j \, w_{ij}}{\sum_j \frac{m_j}{\rho_j} w_{ij}} \tag{7}$$

Another form of obtaining better results is using the continuity equation in the calculation of the density, as can be seen below in equation (8) [47].

$$\frac{d\rho_i}{dt} = \sum_j m_j (v_i - v_j) \, \nabla \mathrm{w}_{ij} \tag{8}$$

There are many forms of calculating the pressure exerted on a particle by the other particles. For high compressibility, an ideal gas equation (9) and the Tait's equation (10) can be used to enforce a very low density variation, leading to an efficient computation [46].

$$P_i = k_p(\rho_i - \rho_0) \tag{9}$$

$$P_i = B((\frac{\rho_i}{\rho_0})^\gamma - 1) \tag{10}$$

where k_p and B are the pressure constants and ρ_0 is the rest density of the fluid and γ is a constant that usually has a value 7 [46].

The pressure force can be calculated using the discretization of the pressure gradient, which will result in (11). This formula is largely used because ensures a modular equality between two particles and conserves linear and angular momentum, increasing the stability in the simulation [47].

$$\frac{1}{\rho_i} \nabla P_i = \sum_j m_j \left(\frac{P_i}{\rho^2{}_i} + \frac{P_j}{\rho^2{}_j} + \Pi_{ij} \right) \nabla \mathrm{w}_{ij} \tag{11}$$

The particle velocities and positions are calculated using a simple time integration, as can be found in the equation (12) and (13), respectively.

$$v_i^{t+1} = v_i^t + a_i^t t \tag{12}$$
$$x_i^{t+1} = x_i^t + v_i^{t+1} t \tag{13}$$

3.1 XSPH

To simulate the viscosity and to prevent particle penetration problem, the XSPH method was used.

The goal of the method is to force particles near each other to move with almost the same velocity. The method is computationally cheaper than other methods and has only one tunable parameter making it easy to change [48].

This parameter controls the viscosity influence on the fluid; the higher the parameter value, the greater the influence of the viscosity on the fluid.

To conserve linear and angular momentum, the formula (14) was used to calculate an intermediate velocity v_i^* and (15) was used to calculate the new velocity.

$$v_i^* = v_i + a_i \nabla t \tag{14}$$

$$v_i = v_i^* + \in \sum_j m_b \frac{(v_i^* - v_j^*)}{\bar{\rho_j}} w_{ij} \tag{15}$$

where a_i is the particle acceleration and $\in$ is the tunable parameter of the XSPH method.

4. RESULTS AND DISCUSSION

In this section, it will be presented the results achieved by applying the XSPH method developed.

To validate the SPH method implemented, we chose four common scenarios to serve as comparison between ours and other SPH variations: The lid-driven cavity problem, the dam break, the Poiseuille flow and the water drop problem. These scenarios have been long used to test and/or validate new developments in the computer fluid dynamics area.

4.1 LID-DRIVEN CAVITY

The lid-driven cavity problem, despite presenting a simple geometric form, develops a flow with relatively complex characteristics. The presence of lid-driven cavities is quite noticeable in engineering problems, consequently, this scenario is widely adopted as test case in numerical modeling research even nowadays.

The test consisted on a flow in a two-dimensional square domain, with three stationary sides and one side having a constant velocity different from zero. It can be better imaginable as a

two-dimensional closed box completely filled with some fluid, as an infinite blade passes over the top of that box. That blade slightly touches the fluid contained in it, placing the fluid in motion, which was initially quiescent [49].

Firstly, the (x, y)-plane was chosen to represent the flow where the x-axis is in the horizontal direction and the y-axis in the vertical direction. The origin is in the bottom left corner of the cavity. The main boundary condition is that the walls must be impermeable, including the ceiling. After applying a constant velocity to the upper edge in the x-axis, a flow would be generated due to the viscosity forces diffusion [50].

In this work, to obtain the results presented below, the square cavity walls were built with a size of $L = 10^{-3}m$, where the number of fluid particles is 1600, making the initial particle spacing be $d = 2.5 * 10^{-5}\, m$. The system organization can be seen in Figure 1. The SPH kernel domain radius was taken as $R = 3 * d$ and the smoothing length h, used in the kernel function, was equal to d. The time step used for the simulation was $\Delta t = 5 * 10^{-5}\, s$.

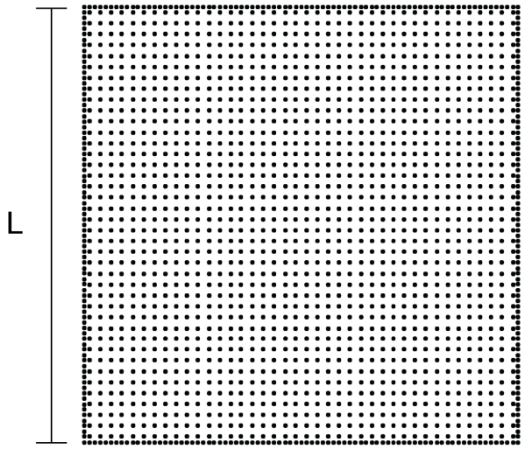

Figure 1. Particles' initial state for the lid-driven cavity simulation.

We determine whether the SPH method used produced satisfactory results by keeping track of the velocities' x-component for the vertical central particles, and the velocities' y-component for horizontal central particles in a specific time step of the simulation. It was observed that at after 2000 time steps ($0.1\, s$) the system began entering in a steady state, so, this time was chosen to be when the particles' information would be extracted.

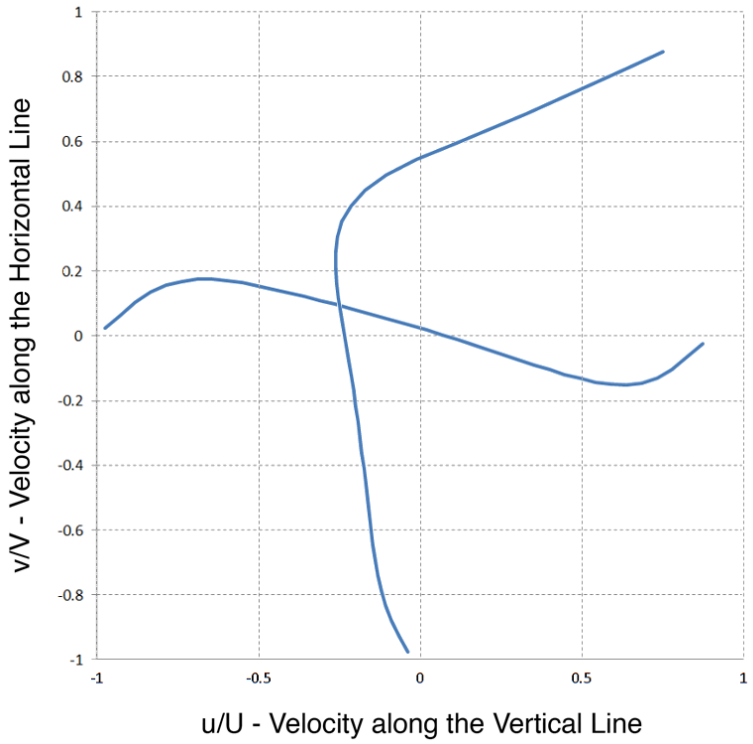

Figure 2. Velocity profiles of the particles in the central lines.

The lines in Figure 2 show the dimensionless velocity values of the central particles after 2000 time steps, with a low viscosity, produced by the XSPH method developed in this work. Compared to [50] and [51] works, these velocity profiles show less smoother curves, which may be caused by density fluctuations of the particles during their calculation.

4.2 DAM BREAK

This problem is useful for testing numerical methods designed for solving flows that have a constant free-surface variation. This scenario was built as a two-dimensional rectangular domain with three stationary sides (bottom, right and left), and a dam, separating two regions of different water heights. This dam bursts right at the first time step of the simulation, at time $t = 0s$. In this test case scenario, the region on the right side of the dam did not contain any water.

As the lid-driven cavity problem, the boundary condition in this scenario is that the walls are impermeable; however, with no top side some particles might escape boundary area (which was not observed during the simulation).

To generate the results presented in this work, the (x, y)-plane was chosen to represent the flow as well, where the x-axis is in the horizontal direction and the y-axis in the vertical one.

The water column had an initial height of $H = 0.6\,m$ and an initial length of $L = 0.6\,m$. The bottom side of the domain had four times the size of L ($2.4\,m$); the model can be seen in Figure 3. The fluid was discretized by using a uniform grid of particles in which the initial particle spacing is $d = 0.01\,m$, that way the total fluid particle number is 3600.
The domain radius was taken as $R = 3 * d$. The smoothing length h was equal to d, as in the lid-driven cavity scenario. The time step length used for the simulation was $t = 10^{-5}\,s$ [52].

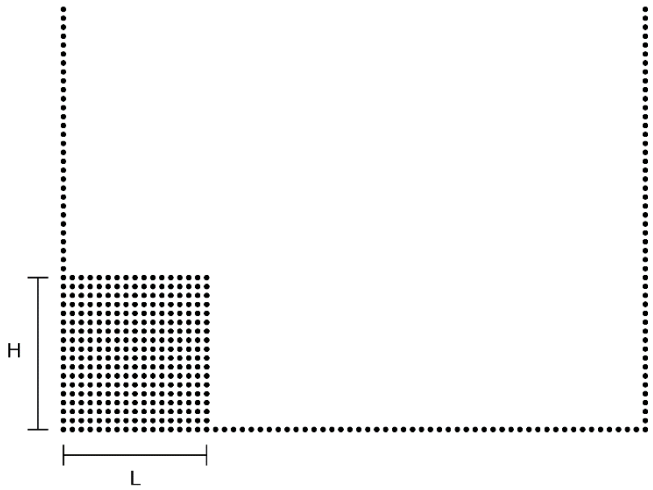

Figure 3. Particles' initial state for the dam break simulation.

To evaluate the XSPH performance in this scenario, we keep track of the propagation of the water wave position right after the dam bursts. The time is represented as a dimensionless value calculated by: $t\sqrt{g/H}$, where t is the time in seconds and g is the gravity in m/s^2. The wave front position is expressed as a function of time and is in a dimensionless form (x/H) as well.

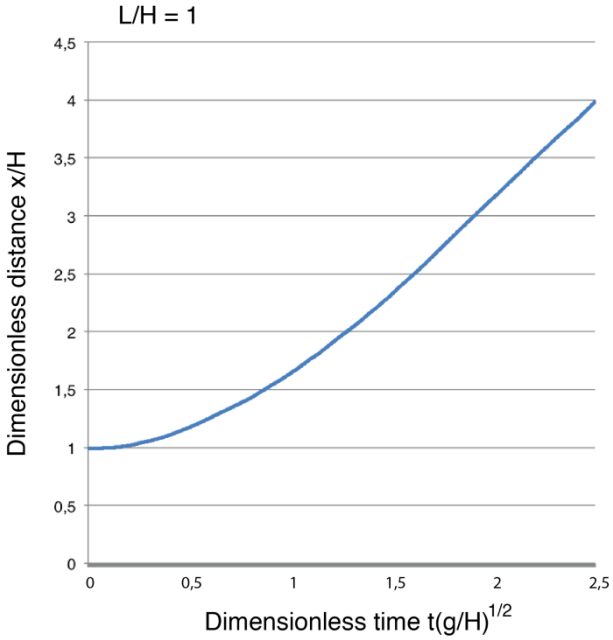

Figure 4. Evolution of the water wave front through dimensionless time.

As depicted in Figure 4, the curve is the result obtained by the XSPH method. If compared with those yielded by the standard SPH, the corrected SPH and with the data extracted from an actual experiment, all found in [52], the method implemented is in very close agreement with them. A valuable observation is that the developed method is more accurate the greater the time is (in this dimensionless time scale).

4.3 POISEUILLE FLOW

A Poiseuille flow is generally known as an unsteady viscous fluid flow driven by the presence of an effective pressure gradient between the two ends of a long straight pipe of uniform circular cross-section. It is an interesting test to check the accuracy and reliability of the proposed method.

Again, to generate the results presented in this work, the (x, y)-plane was chosen to represent the flow, the x-axis is in the horizontal direction and the y-axis in the vertical direction. To simulate the infinite pipe, the implementation was done so that the particles leaving the pipe section would return to the pipe's entrance in its same position (relative to y-axis), while its speed relative to the x-axis would be reduced back to the v_0 that all particles are submitted in the very first step of the simulation [45].

The calculations in this method were made using 800 particles. The pipe was modeled with two plates, one in $y = 0\,m$ and the other in $y = 10^{-3}\,m$, in other words, a height $H =$

$10^{-3}\,m$. Both plates have a width $L = 5 * 10^{-4}\,m$ (between $x = 0\,m$ and $x = 5 * 10^{-4}\,m$). Hence, the distance between the two plates is two times larger than (one of) the plate's size; that space between them is where the fluid passes through, as shown in Figure 5. The particles are arranged in a rectangular format, with 20 particles along the length L and 40 particles along H, yielding an initial particle spacing of $d = 2.5 * 10^{-5}\,m$. The domain radius was chosen $R = 3 * d$ and the time step utilized was $t = 10^{-5}\,s$ [25].

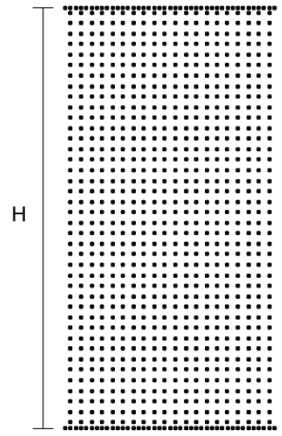

Figure 5. Particles' initial state for the Poiseuille flow simulation.

It is important to note that all walls and boundaries, not only in this simulation, but also in both previous scenarios, are formed by particles (the same particles that form the fluid). Of course, boundary particles have different physical characteristics from the fluid particles.

To evaluate the performance of the proposed method in this scenario, it is presented in Figure 6 the velocity profiles of a vertical line of particles at certain times from the beginning of the simulation until 1.0 s, which is when the velocity profile reaches a steady-state regime.

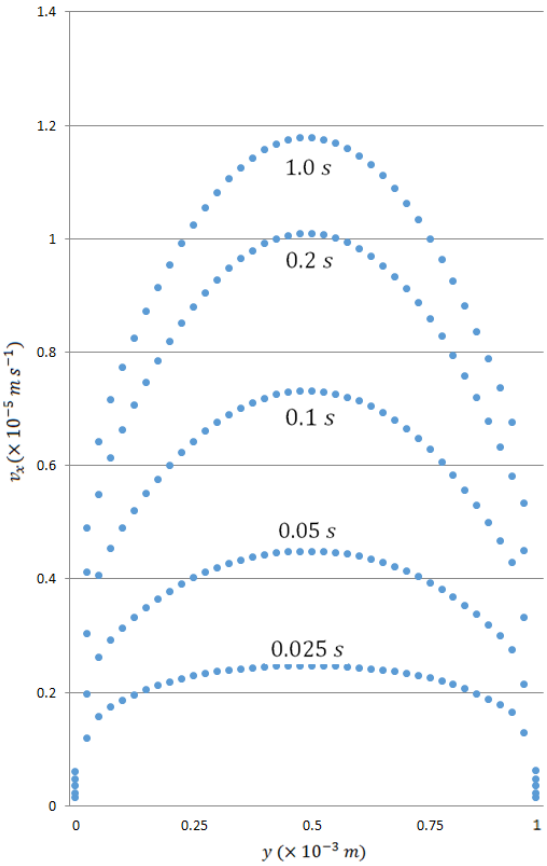

Figure 6. Numerical solution of the Poiseuille flow generated by the proposed method.

In Figure 6 the dots represent the numerical solution of the Poiseuille flow produced by the implemented method. Comparing it to the analytical solution of the Poiseuille flow and to the numerical solution in [25], is possible to see our method's precision since it is in close agreement with both other approaches.

4.4 ELLIPTIC DROP

The examination of the evolution of an elliptic water drop is generally one of the first scenarios to test the accuracy of a newly developed fluid simulation method and one of most traditional ways to verify it. A notable example of its use is in Monaghan's work on free surface flows [33].

The (x, y)-plane was chosen to represent the flow once again, where the x-axis is in the horizontal direction and the y-axis in the vertical one. The usual test consists on a two-dimensional water drop, beginning as a circle (seen in Figure 7), with a predefined velocity field so that the drop keeps its elliptic shape over time. The circle radius is $1\ m$ and the initial particle spacing is $d = 0.05\, m$ in both directions, implying a total of 1256 particles. The

domain radius was taken as $R = 3 * d$. Each particle has a mass of $m = 2.5\,kg$ and the time step used for the simulation was $t = 10^{-5}\,s$ [53].

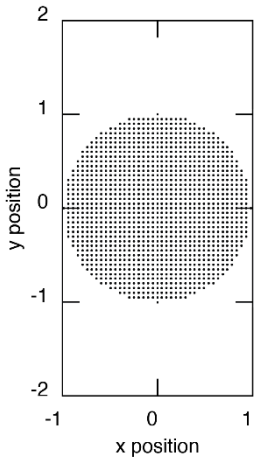

Figure 7. Particles' initial state for the elliptic drop simulation.

In Figure 8, it can be seen the evolution through time of the water drop. The circular drop turns into an ellipse. This ellipse major axis, which grows in the y-axis direction, reaches a size of $1.82\,m$ in $0.0082\,s$.

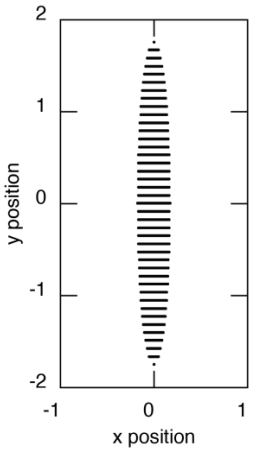

Figure 8. Particles' state after $0.0082\,s$.

Although the elliptic drop simulation presents a coherent and visually realistic output, the elliptic drop major axis cannot successfully reach two times its initial radius, which is the main objective in this scenario. Again, this happens due to the lack of control when calculating the particles' density, which has to, ideally, remain constant or at least not having any large variations.

5. CONCLUSIONS

This paper compares four test cases with the results found in the bibliography using the weakly compressible SPH method: lid-driven cavity, dam break, Poiseuille flow and elliptic drop.

The results found were visually coherent and analytically precise in most of the cases, which include tests with free surface and with boundaries.

The XSPH method demonstrated to be coherent to simulate viscosity and boundary forces, keeping particles near each other with close velocity and preventing the particles to outdistance the boundary wall. But, the method couldn't create a simulation with complete numerical accuracy because it is a mathematical tool to create a real physical force, which shows good agreement with the results obtained by [48]. The viscosity effect can be better represented, for instance, using the artificial viscosity model found in [54].

A problem found in the algorithm was the calculation of the density in case of a truncated kernel or in cases of a low number of particles in the whole simulation, creating a region of instability because the density does not reach values close to the rest density.

This work can be improved in many ways. The first improvement is to simulate the scenarios with a bigger number of particles to overcome the density problem found in some test cases, and the next step is to improve the method implemented to simulate cases in 3D dimensions.

Other test cases can be simulated, for instance, adding rigid bodies into the fluid [55], mixing two fluids with different densities [56] or adding the turbulence factor into the simulation, which would allow to simulate scenery with a larger Reynolds number [57].

Different from a mesh based method, the SPH has an independence in operations over the particles. Due that independence, the method is easily parallelizable, which would decrease the computation time of an interaction creating the possibility of simulations with a bigger number of particles with a relative small time of computation and creating simulations in real time.

REFERENCES

[1] P.W. Cleary et al, "Novel applications of smoothed particle hydrodynamics (SPH) in metal forming", *Journal of Materials Processing Technology*, Vol. **177**, pp. 41-48, (2006).

[2] T. Belytschko et al, "Meshless Methods: An Overview and Recent Developments", *Computer Methods in Applied Mechanics and Engineering*, Vol. **139**, pp. 3-47, (1996).

[3] L.B. Lucy, "A numerical approach to the testing of the fission hypothesis", *Astronomical Journal*, Vol. **82**, pp. 1013-1024, (1977).

[4] R.A. Gingold and J.J. Monaghan, "Smoothed particle hydrodynamics – Theory and application to non-spherical stars", *Monthly Notices of the Royal Astronomical Society*, Vol. **181**, pp. 375-389, (1977).

[5] I. Babuška et al, "Survey of Meshless and Generalized Finite Element Methods: A Unified Approach", *Acta Numerica*, Vol. **12**, pp. 1-125, (2003).
[6] J. Orkisz, *Finite Difference Method (Part III)*, Handbook of Computational Solid Mechanics, Springer-Verlag, pp. 336-432, (1998).
[7] J. Orkisz and J. Krok, "On Classification of the Meshless Methods", *8th World Congress on Computational Mechanics*, (2008).
[8] K. Szewc et al, "Analysis of the incompressibility constraint in the smoothed particle hydrodynamics method", *International Journal for Numerical Methods in Engineering*, Vol. **92**, pp. 343-369, (2012).
[9] M.S. Shadloo et al, "A robust weakly compressible SPH method and its comparison with an incompressible SPH", *International Journal for Numerical Methods in Engineering*, Vol. **89**, pp. 939-956, (2012).
[10] E.-S. Lee et al, "Application of weakly compressible and truly incompressible SPH to 3-D water collapse in waterworks", *Journal of Hydraulic Research*, Vol. **48**, pp. 50-60, (2010).
[11] S. Børve, "Generalized Ghost Particle method for handling reflecting boundaries", *6th International SPHERIC Workshop*, (2011).
[12] S. Marrone, "Enhanced SPH Modeling of free-surface flows with large deformations", *Phd Thesis, Università di Roma*, (2011).
[13] B. Song and L. Dong, "A new boundary treatment method for SPH and application in fluid simulation", *3rd International Conference on Information and Computing*, Vol. **4**, pp. 82-85, (2010).
[14] M. Yildiz et al, "SPH with the multiple boundary tangent method", *International Journal for Numerical Methods in Engineering*, Vol. **77**, pp. 1416-1438, (2009).
[15] J. Feldman and J. Bonet, "Dynamic refinement and boundary contact forces in SPH with applications in fluid flow problems", *International Journal for Numerical Methods in Engineering*, Vol. **72**, pp. 295-324, (2007).
[16] S.J. Cummins and M. Rudman, "An SPH Projection Method", *Journal of Computations Physics*, Vol. **152**, pp. 584-607, (1999).
[17] A. Ghasemi et al, "2D numerical simulation of density currents using the SPH projection method", *European Journal of Mechanics B/Fluids*, Vol. **38**, pp. 38-46, (2013).
[18] R. Xu et al, "Accuracy and stability in incompressible SPH (ISPH) based on the projection method and a new approach", *Journal of Computational Physics*, vol. **228**, pp. 6703-6725, (2009).
[19] D.L. Brown et al, "Accurate Projection Methods for the Incompressible Navier–Stokes Equations", *Journal of Computational Physics*, Vol. **168**, pp. 464-499, (2001).
[20] M. Asai et al, "A Stabilized Incompressible SPH Method by Relaxing the Density Invariance Condition", *Journal of Applied Mathematics*, Vol. **2012**, 24 pages, (2012).
[21] J. Pozorski and A. Wawreńczuk, "SPH Computation of Incompressible Viscous Flows", *Journal of Theoretical and Applied Mechanics*, Vol. **40**, pp. 917-937,

(2002).
[22] E.-S. Lee et al, "Comparisons of weakly compressible and truly incompressible algorithms for the SPH mesh free particle method", *Journal of Computational Physics*, Vol. **227**, pp. 8417-8436, (2008).
[23] S.J. Watkins et al, "A new prescription for viscosity in Smoothed Particle Hydrodynamics", *Astronomy & Astrophysics Supplement Series*, Vol. **119**, pp. 177-187, (1996).
[24] A. Rafiee et al, "An incompressible SPH method for simulation of unsteady viscoelastic free-surface flows", *International Journal of Non-Linear Mechanics*, Vol. **42**, pp. 120-1223, (2007).
[25] L.D.G. Sigalotti et al, "SPH simulations of time-dependent Poiseuille flow at low Reynolds numbers", *Journal of Computational Physics*, Vol. **191**, pp. 622-638, (2003).
[26] X. Yang et al, "Smoothed particle hydrodynamics modeling of viscous liquid drop without tensile instability", *Computers & Fluids*, Vol. **92**, pp. 199-208, (2014).
[27] M. Ferrand et al, "Unified semi-analytical wall boundary conditions for inviscid, laminar or turbulent flows in the meshless SPH method", *International Journal for Numerical Methods in Fluids*, Vol. **71**, pp. 446-472, (2013).
[28] J.R. Shao et al, "An improved SPH method for modeling liquid sloshing dynamics", *Computers and Structures*, Vol. **100-101**, pp. 18-26, (2012).
[29] J.W. Swegle et al, "Smoothed Particle Hydrodynamics Stability Analysis", *Journal of Computational Physics*, Vol. **116**, pp. 123-134, (1995).
[30] J. Bonet and S. Kulasegaram, "A simplified approach to enhance the performance of smooth particle hydrodynamics methods", *Applied Mathematics and Computation*, Vol. **126**, pp. 133-155, (2002).
[31] J. Bonet and T.-S.L. Lok, "Variational and momentum preservation aspects of Smooth Particle Hydrodynamic formulations", *Comput. Methods Appl. Mech. Engrg*., Vol. **180**, pp. 97-115, (1999).
[32] M.B. Liu and G.R. Liu, "Smoothed Particle Hydrodynamics (SPH): an Overview and Recent Developments", *Arch. Comput. Methods. Eng.*, Vol. **17**, pp. 25-76, (2010).
[33] J.J. Monaghan, "Simulating Free Surface Flows with SPH", *Journal of Computational Physics*, Vol. **110**, pp. 399-406, (1994).
[34] B. Ataie-Ashtiani et al, "Modified incompressible SPH method for simulating free surface problems", *Fluid Dynamics Research*, Vol. **40**, pp. 637-661, (2008).
[35] A. Bøckmann et al, "Incompressible SPH for free surface flows", *Computers & Fluids*, Vol. **67**, pp. 138-151, (2012).
[36] A.J.C. Crespo, "Application of the Smoothed Particle Hydrodynamics model SPHysics to free-surface hydrodynamics", *Phd Thesis, Universidade de Vigo*, (2008).
[37] J. Fang et al, "Improved SPH methods for simulating free surface flows of viscous fluids", *Applied Numerical Mathematics*, Vol. **59**, pp. 251-271, (2009).
[38] A. Kiara, "SPH for incompressible free-surface flows. Part I: Error analysis of the basic assumptions", *Computers & Fluids*, Vol. **86**, pp. 611-624, (2013).
[39] T. Harada et al, "Improvement in the Boundary Conditions of Smoothed Particle Hydrodynamics", *Computer Graphics & Geometry*, Vol. **9**, pp. 2-15, (2007).

[40] M. Lastiwka et al, "Permeable and Non-reflecting Boundary Conditions in SPH", *International Journal for Numerical Methods in Fluids*, Vol. **61**, pp. 709-724, (2009).
[41] J.J. Monaghan and J.B. Kajtar, "SPH particle boundary forces for arbitrary boundaries", *Computer Physics Communications*, Vol. **180**, pp. 1811-1820, (2009).
[42] X.Y. Hu and N.A. Adams, "A multi-phase SPH method for macroscopic and mesoscopic flows", *Journal of Computational Physics*, Vol. **213**, pp. 844-861, (2006).
[43] A. Zainali et al, "Numerical investigation of Newtonian and non-Newtonian multiphase flows using ISPH method", *Comput. Methods Appl. Mech. Engrg*, Vol. **254**, pp. 99-113, (2013).
[44] J.J. Monaghan, "SPH without a Tensile Instability", *Journal of Computational Physics*, Vol. **159**, pp. 290-311, (2000).
[45] J.P. Morris, P.J. Fox and Y. Zhu, "Modeling Low Reynolds Number Incompressible Flows Using SPH", *Journal of Computational Physics*, Vol. **136**, pp. 214-226, (1997).
[46] J.J. Monaghan, "Smoothed particle hydrodynamics", *Reports on progress in physics*, Vol. 68, n. 8, pp. 1703, (2005).
[47] J.J. Monaghan, "Smoothed particle hydrodynamics", *Annual review of astronomy and astrophysics*, Vol. **30**, pp. 543-574, (1992).
[48] H. Schechter, R. Bridson, "Ghost SPH for animation water", *ACM Transactions on Graphics (TOG)*, Vol. **31**, n. 4, (2012).
[49] J.D. Bozeman and C. Dalton, "Numerical Study of viscous flow in a cavity", *Journal of Computational Physics*, Vol. **12**, pp. 348-363, (1973).
[50] W.J.N. Pinto, "Aplicação do método lagrangiano SPH para a solução do problema das cavidades", *Master's Thesis, Universidade Federal do Espírito Santo*, (2013).
[51] S. Chantasiriwan, "Performance of Multiquadric Collocation Method in Solving Lid-driven Cavity Flow Problem with Low Reynolds Number", *Computer Modeling In Engineering & Sciences*, Vol. **15**, n. 3, pp. 137-146, (2006).
[52] R. Staroszczyk, "Simulation of Dam-Break Flow by a Corrected Smoothed Particle Hydrodynamics Method", *Archives of Hydro-Engineering and Environmental Mechanics*, Vol. **57**, n. 1, pp. 61-79, (2010).
[53] J. Pelfrene, "Study of the SPH method for simulation of regular and breaking waves", *Master's Thesis*, *Universiteit Gent*, (2011).
[54] M. Becker and M. Teschner, "Weakly compressible SPH for free surface flows", *Proceedings of the 2007 ACM SIGGRAPH/Europgraphics symposium on Computer animation. Eurographics Association*, (2007).
[55] N. Akinck et al, "Versatile rigid-fluid coupling for incompressible SPH", *ACM Transactions on Graphics (TOG)*, Vol. **31**, n. 4, (2012).
[56] B. Solenthaler and R. Pajarola, "Density Contrast SPH Interface", *ACM SIGGRAPH/Eurographics Symposium on Computer Animation*, (2008).
[57] J.J. Monaghan, "A Turbulence Model for Smoothed Particle Hydrodynamics", *European Journal of Mechanics-B/Fluids*, Vol. **30**, n. 4, pp. 260-370, (2011).